*Special Conference Edition, April, 2022*
http://dx.doi.org/10.4314/bajopas.v13i1.86S
***Bayero Journal of Pure and Applied Sciences, 13(1): 576 - 581***
**ISSN 2006 – 6996**

# EXPERIMENTAL CHARACTERIZATIONS OF MICRO-ARRAY OF BINARY FRESNEL LENSES FABRICATED BY ELECTRON BEAM LITHOGRAPHY

**Chiromawa, N.L.**
Department of Physics, Umaru Musa Yar'adua University, P. M. B. 2218 Katsina, Nigeria
Contacts: nchiromawa@gmail.com, +2348035944145

***ABSTRACT***
***In this paper, Micro-scale Fresnel lenses array were fabricated by exposing electron beam on poly (methyl methacrylic) PMMA, photoresist in the region between $R_{2Z-1/3}$ and $R_{2Z}$ on $SiO_2$ substrate, where $Z = 1, 2, \ldots \ldots 11$. Each unit of these Fresnel lenses has a maximum external diameter of $40.58 \mu m$, a Focal length of $45.197 \mu m$ and the $f$-number of $1.11$. The total number of rings of this Fresnel lens is $11$ and its grating pitch on the periphery is $680\ nm$. High transmission efficiency of 93.7% was obtained at the wavelength of 650 nm for the thickness of the PMMA, photoresist of 250 nm.***
***Keywords: Micro-Fresnel lens, Focal length, EBL, $SiO_2$, PMMA.***

## INTRODUCTION

*Micro-lenses* have been widely used for application in various optical systems such as data recording and retrieval systems, high-speed detectors, as well as integrated micro-optical systems, among others (Arbabi *et al*., 2015). In particular, micro-scale Fresnel lens (MSFL) plays important role in many applications, such as focused laser diode beam (Hasan and Lee, 2015), Concentration photovoltaic systems (Li *et al*., 2015; Xie *et al*., 2015) and Optical interconnection (Gu *et al*., 2015).

There are many methods employed to fabricate MSFL, these include; Micro-Electro-Mechanical Systems (MEMS) fabrication process (Tsui *et al*., 2012), Electron beam lithography EBL (Teruo Fujita *et al*., 1981) and Photolithography (Yu *et al*., 2015). Fresnel lens fabricated by EBL process offers more advantages over Fresnel lens fabricated by other techniques. These advantages include (Kley, 1997; T Fujita *et al*., 1982): Lenses with précis dimensions can be fabricated, Lens parameters such as diameter, focal length, wavelength and F-number can easily be changed, spherical aberrations can be reduced to the nearest minimum by optimizing the exposure conditions and the reliefs of the lens can easily be copied, hence, can be used for many optical and electronics applications. In this paper, we designed, fabricated and characterized a micro-scale Fresnel lens on $SiO_2$ wafer using electron-beam lithography EBL, process for optical and electronics applications. To minimize the reflection and simultaneously enhances the absorption of incident light, we used 680 nm as the electron beam diameter which is smaller than the wavelength of the band-gap energy of the silicon and its associated materials (Chiromawa and Ibrahim, 2016b; Chiromawa and Ibrahim, 2016a). Because of its good compatibility with silicon and its dielectrics, as well as the fact that it provides good adhesion, mechanical properties and optical clarity (Chiromawa and Ibrahim, 2014; Chiromawa and K. Ibrahim, 2015b), PMMA was chosen as a photoresist for the electron beam lithography EBL. Another important property that attracted our attention to use the PMMA is that it is used in the MEMS process as a positive photoresist to provide high-contrast and high-resolution images (C. Vieu *et al*., 2000; Chiromawa and Ibrahim, 2015).

## MATERIALS AND METHODS

The methodology adopted in this paper begins with the optical design and simulation of the Fresnel lens followed by the fabrication and characterization processes.

### *Optical Design and Simulation*

To design a Fresnel lens, the fundamental parameters that determine the optical properties of the lens and the mathematical relationships linking these parameters are considered first. The parameters include; aperture size of the lens, wavelength, focal length, and refractive index, among others (Davis, 2011). We define the *relative aperture or f-number* in the following equation;

$$f - number = \frac{f}{D} \qquad (1)$$

Where; $f$ is the focal length, and $D$ is the aperture diameter of the lens.

Since; the Fresnel lens' structure composes of concentric circular rings at different depths; the *radius* of the $z^{th}$ ring $r_z$, can be expressed by the following equation;

$$r_z = \sqrt{z\lambda f} \qquad (2)$$

Where, $z$ is the number of a ring, $f$ is the focal length, and $\lambda$ is the wavelength.

For an incident plane wave, the intensity distribution on the focal plane can be expressed by an Airy distribution function (Majumdar and Comtet, 2005), therefore if $\theta$ is the angle between the axis of the lens aperture and the line between lens' optical center and eye piece, $J_1$ is the first order Bessel function, and R is the lens' aperture radius. Then the intensity distribution $I_\theta$ is given by equation (3):

$$I_\theta \approx I_o \left|\frac{2J_1(kRsin\theta)}{kRsin\theta}\right|^2 \qquad (3)$$

Where $I_o$ the maximum intensity of the Fresnel rings pattern at the lens' optical centre and k is the wave number.

On the other hand, light passing through the lens bends. Hence, the depth $h$, at which the light (of wave number $k = \frac{2\pi}{\lambda}$) passed through a medium of refractive index $n$, can be obtained by the equation; $knh - kh = 2\pi$, which can further be simplified to obtained $h$ as follows;

$$h = \frac{\lambda}{(n-1)} \qquad (4)$$

The refractive index for a given medium of wavelength $n_\lambda$ can be found by the Snell's law of refraction in the following equation;

$$n_\lambda = \frac{n_A sin\theta_i}{sin\theta_t} \qquad (5)$$

Where; $\theta_t$ is the refracted angle due to the medium, $\theta_i$ is incident angle due to air medium and $n_A = 1$ is the refractive index of air. Depending on the material medium used, the refractive index $n$, is almost constant for any given material medium, and is related to the wavelength $\lambda$ equation (5). For micro-scale Fresnel lens with rectangular grooves fabricated by electron-beam lithography with the PMMA resist thickness $h$, the efficiency of generating $i^{th}$ order ($i = \pm 1, \pm 2, \pm 3, \dots\dots\dots..$) diffraction waves could be related to their diffraction efficiency. Then the diffraction efficiency $\eta_i$ can be expressed by equation (6):

$$\eta_i = \frac{4}{i^2\pi^2} sin^2\left(\frac{\pi h(n-1)}{2\lambda cos\vartheta}\right) sin^2(n\pi\delta) \qquad (6)$$

Where; $n$ is the refractive index of PMMA, $\lambda$ is the wavelength of light, $\vartheta$ is the angle of incident light and $\delta$ is the duty ratio. On the other hand, for the same micro-scale Fresnel lens with an asymmetric saw-tooth shape, the diffraction efficiency of $m^{th}$ order diffraction waves can be expressed by the following equation;

$$\eta_m = \{\frac{1}{T}\int_0^T e^{(i\varphi_{(x)})} e^{(-j\frac{2\pi mx}{T})} dx\}^2 \qquad (8)$$

Where $T$ is the grating period, $\varphi_{(x)}$ is the phase-retardation function of the grating and m is the diffraction order ($m = \pm 0, \pm 1, \pm 2, \pm 3 \dots\dots\dots\dots\dots$). In this paper, the Fresnel rings were designed using GDSII Editor contained in Raith-ELPHY Quantum software. The GDSII Editor is sub-software built in the Raith-ELPHY Quantum software, and it is used for designing many geometrical shapes such as rectangles, circles and curvatures, lines and dots as well as other polygons in separated layers for multilevel exposure (Raith Softsware, 2007), while the formation of Fresnel rings (or pattern generation) on the layer of PMMA was achieved using Scanning electron microscopy (SEM) JEOL JSM-6460LV with Raith-ELPHY Quantum for EBL system (NOR, USM). The designed Fresnel lens consists of eleven concentric circular rings expanding symmetrically from the optical center. The diameter of the first Fresnel ring is $\approx 5\,\mu m$, while the diameter of eleventh Fresnel ring is $\approx 52\,\mu m$. The relative aperture or $f - number$ was designed to be $\approx 1.26\,\mu m$ at the wavelength of $700\,nm$, and the thickness of each ring is assumed to be $\approx 500\,nm$.

***Fabrication and Characterization Processes***

$1cm^2$ $SiO_2$ substrate was cleaned using particles decontamination DECON procedures by having immersed in the mixture of $(H_2SO_4 + H_2O_2)$ solution in the ratio of $(3:1)$ at the temperature of $110^oC$ for about 15 to 20 min. $SiO_2$ was then removed and inserted in DI water at the temperature of $80^oC$ and rinsed with DI water. Finally, the substrate was dried with Nitrogen gas ($N_2$). To increase the adhesive force between $SiO_2$ and PMMA interface; before spin coat process, the plasma treatment was additionally done on the surface of $SiO_2$ (Karamdel *et al.*, 2011). Meanwhile, to obtain 200 nm thickness of PMMA resist layer on $SiO_2$ wafer (Nurul and Ahmad, 2006), the wafer was spun coat at 4000 rpm rotational speeds for 90 sec. using a spin coater. To ensure the total dryness and off-gassing, the sample was baked in an oven at a temperature $180^oC$ for $60$ mins. To prevent charge-up during electron beam exposure, a very thin layer of platinum Pt, was deposited on $SiO_2$ substrate using a Rotary pumped sputter coater (Model: Q150R S).

The EBL process was then used to define a circular pattern of Fresnel rings on the layer of PMMA. After exposure, the metal layer was removed by etching using the ICP-RIE system (model: Oxford Plasmalab 80 Plus) and the electron beam exposed layer of PMMA was developed in a mixture of Methyl Isobutyl Ketone MIBK, and Isopropyl Alcohol IPA, (MIBK:IPA) in the ratio of 1:3 (by volume) at the temperature of $23^oC$ for $35\ \mathrm{sec}$. The wafer was then inserted in to the solution of IPA for the duration of $35\ \mathrm{sec}$. as a stopper. Finally, the sample was then dried by blowing it with nitrogen and the developed structures were characterized using Field Emission Scanning Electron Microscope FESEM and EDS/EBSD detector system (model: FEI Nova NanoSEM 450) and the Atomic Force Microscope AFM, (Dimension EDGE, BRUNKER; Shimadzu) system. Table 1 shows the EDX result of PMMA/$\mathrm{SiO_2}$ surface obtained from the EDX analysis, figure 1 shows a FESEM image of the developed structures of PMMA/$SiO_2$ Fresnel rings at different magnifications, while figure 2 shows the AFM analysis of the fabricated Fresnel lens on $SiO_2$.

Table 1**:** EDX results of PMMA film layer spun coat on $SiO_2$

| S/N | Sample | Elements (Weight %) | | | |
|---|---|---|---|---|---|
| | | Si | O | C | F |
| 1 | $SiO_2$ | 44.07 | 55.93 | 0.00 | 0.00 |
| 2 | $SiO_2$ etched | 45.72 | 54.12 | 0.05 | 0.11 |
| 3 | PMMA/$SiO_2$ | 31.62 | 36.64 | 31.65 | 0.09 |

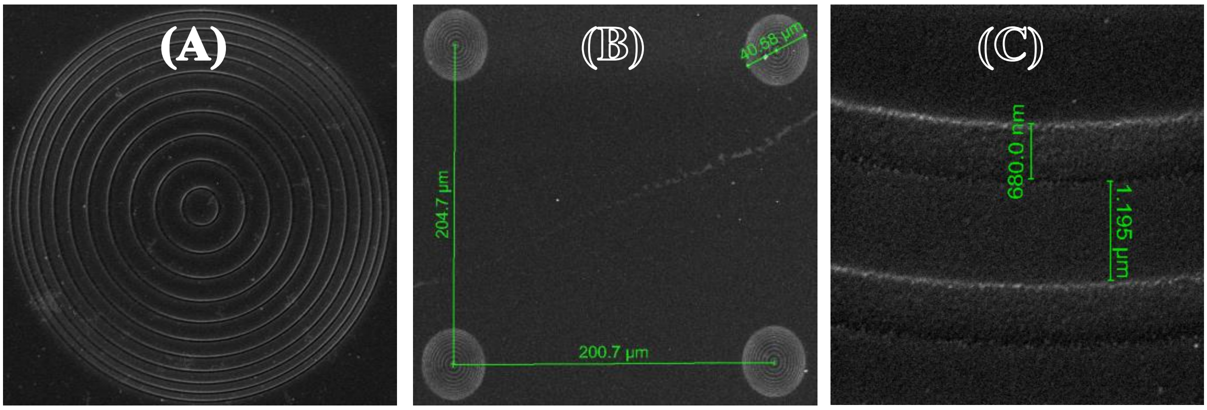


Figure 1: FESEM images of $\mathrm{PMMA/SiO_2}$ Fresnel lenses at different magnifications (a) 5000X (b) 800X and (c) 30KX.

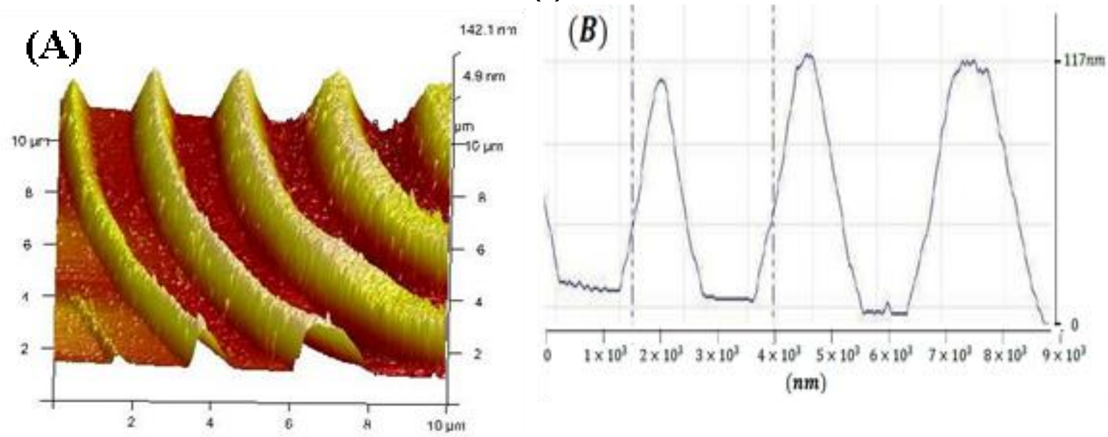


Figure 2: AFM images of Fresnel lenses on $\mathrm{SiO_2}$; (a) 3-D view of AFM image (b) AFM analysis of lens' facet profile.

## RESULTS AND DISCUSSION

As seen in figure 1: each unit of Fresnel lens consists of eleven concentric circular fringes with an external diameter of 40.58 um. However, the dimensions of the Fresnel rings radius shrunk from the designed dimensions. These errors may occur due to some factors associated with the electron beam exposure or EBL process. Figure 3 (a) shows the plot of Fresnel rings' radius against number of Fresnel zone Z, with the graphical relationship of the errors that occurred at each Fresnel zone.

Furthermore, the occurrence of these errors affects the dimension of focal length, or in other words; due to these errors, the focal length $f_D$ of the designed Fresnel lens differs from that of measured focal length $f_M$. However, in both cases the focal length varies with the variations of the wavelength. Figure 3 (b) shows the plot of focal length against wavelength of visible light with the graphical representation of the differences between the designed and measured focal lengths. According to the FESEM analysis, the thickness of each ring is about $680\ \mathrm{nm}$ (as depicted in figure 1 (c)) which means that the beam diameter (during EBL process) has increased due to the electrons scattering. The vertical distance between the centre of each Fresnel lens unit is $204.7\ \mu\mathrm{m}$, while the horizontal distance is about $200.7\mu\mathrm{m}$ (refer to Fig. 1 (b)). In figure 2, the diameter of each ring can be obtained by multiplying its radius by a factor of 2. The outermost ring has an approximate diameter of $40.58\ \mu\mathrm{m}$ and the innermost ring has a diameter of about $3.64\ \mu\mathrm{m}$ (Figure 1 (b)). The separation between each ring decreases by a factor of $0.478\ \mu\mathrm{m}$ starting from the innermost ring. This is consistent with the Fresnel lens design technique (Chiromawa and Ibrahim, 2015a). However, the AFM analysis of the sample shows that the Fresnel rings have a binary profile with the approximate depth of about 87 nm and the root-mean-square surface roughness of about 1.9 nm as depicted in figure 2 c.

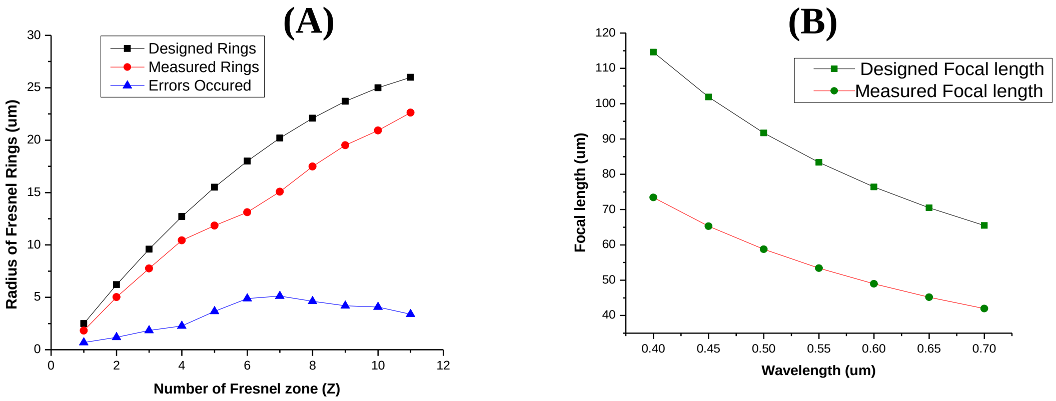


Figure 3: (a) Plot of Fresnel rings' radius against number of Fresnel zone Z, with a graphical relationship of the errors that occurred at each Fresnel zone and (b) Graphical relationship comparing the designed and measured focal lengths of Fresnel lens against the wavelength of visible light.

The intensity distribution on the focal plane was measured using an Optical microscope (Model: BA310) by replacing the light source with the light-emitting diode LED having the same rate of power as that of the halogen lamp. The optical microscope analysis for the intensity distribution on the focal plane could be represented by figure 4. Each height of the Airy distribution function represents the intensity at the focal plane. The highest intensity corresponds to the focal plane at $\approx 45\ \mu\mathrm{m}$ showing that the focal point is located at $\approx 45.20\ \mu\mathrm{m}$ from the plane of the lens. Therefore, this Fresnel lens has $f$-number of $\approx 1.11$ at the wavelength of $650\ \mathrm{nm}$. The effective transmission decreases with the increase in the incidence angle (Figure 5). The highest transmission efficiency ($\approx 94\%$) corresponds to the smallest incident angle was achieved at $\theta_i \approx 0^o$.

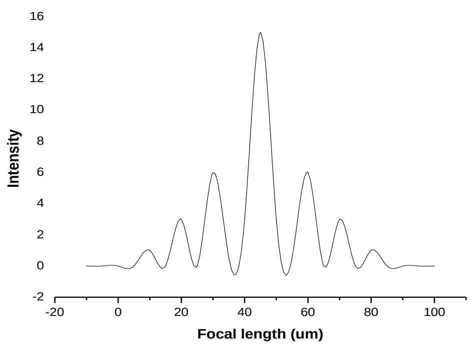


Figure 4: Graphical representation of the intensity distribution on the focal plane.

**CONCLUSION**

In this paper, we have successfully fabricated the array of $SiO_2$ Fresnel lenses using the EBL process. The results demonstrated that Fresnel lens units containing eleven concentric rings were created on the PMMA layer with the outermost Fresnel ring having the maximum diameter of $40.58\ \mu m$ and they are horizontally located $200.7 \mu m$ and vertically $204.7 \mu m$ apart. The optical analysis shows that the Fresnel lens has an approximate focal length of $45\ \mu m$ and an approximate $f-number$ of $1.11$. The transmission efficiency of $93.7\%$ was achieved at an incident angle of $0^o$. Thus conclusively, the above features could be utilized as an array of micro-scale Fresnel lenses for micro-optics, in particular, couplers between laser diodes and optical fibres, and pick-up lenses from optical fibres as well as micro lenses for concentrator photovoltaic application especially for crystalline silicon solar cells.

**REFERENCES**


Arbabi, A., Horie, Y., Ball, A. J., Bagheri, M., and Faraon, A. (2015). *Efficient high NA flat micro-lenses realized using high contrast transmitarrays.* Paper presented at the SPIE OPTO.

C. Vieu, F. Carcenac, A. Pe´pin, Y. Chen, M. Mejias, A. Lebib, . . . Launois, H. (2000). Electron beam lithography: resolution limits and applications. *Applied Surface Science 164 (2000) 111–117 Elsevier*.

Chiromawa, N., and Ibrahim, K. (2015). Effects of poly (methyl methacrylate) PMMA, film thickness in the Light Transmission through SiO2 for Applications in Solar Cells Technology. *International Journal of Engineering and Innovative Technology, 5*(1), 125-131.

Chiromawa, N. L., and Ibrahim, K. (2014). *Infrared Transmission through PMMA/SiO₂ for the Applications in Solar cells Technology: Fourier Transform Infra-red (FTIR) Spectroscopy.* Paper presented at the International Conference of Global network for Innovative Technology (IGNITE 2014), Pinang Malaysia.

Chiromawa, N. L., and Ibrahim, K. (2015a). Concept of Bee-eyes array of Fresnel lenses as a solar photovoltaic concentrator system. *Journal of Photonics, 2015*, 6. doi: 10.1155/2015/327342.

Chiromawa, N. L., and Ibrahim, K. (2015b). Surface investigations and study optical properties of Si and SiO2 substrates-coated with Poly (methyl methacrylate) PMMA for high efficiency solar cells. *Australlian Journal of Basic and applied Science*(Special issue 9 (12)), 12-17.

Chiromawa, N. L., and Ibrahim, K. (2016a). *Design and Fabrication of PMMA/SiO₂ Micro Array Of Binary Fresnel lenses by Electron Beam Lithography.* Paper presented at the International Sciences, Technolgy and Engineering Conference, Advanced Materials Chemistry and Physics (ISTEC 2016), Equatorial Hotel Penang, Malaysia.

Chiromawa, N. L., and Ibrahim, K. (2016b). Fabrication of micro-array of Fresnel rings on Si by electron beam lithography and reactive ion etching. *Applied Physics A, 122*(2), 1-8.

Davis, A. (2011). *Fresnel lens solar concentrator derivations and simulations.* Paper presented at the SPIE Optical Engineering+ Applications.

Fujita, T., Nishihara, H., and Koyama, J. (1981). Micro Fresnel lenses fabricated by electron-beam lithography. *Electronics and Communications in Japan (Part I: Communications), 64*(10), 104-110.

Fujita, T., Nishihara, H., and Koyama, J. (1982). Blazed gratings and Fresnel lenses fabricated by electron-beam lithography. *Optics letters, 7*(12), 578-580.

Gu, Z., Amemiya, T., Ishikawa, A., Kang, J., Hiratani, T., Hayashi, Y., . . . Arai, S. (2015). Investigation of Optical Interconnection by Using Photonic Wire Bonding. *Journal of Laser Micro/Nanoengineering*.

Hasan, M. N., and Lee, Y.-C. (2015). Beam pen lithography based on focused laser diode beam with single microlens fabricated by excimer laser. *Optics Express, 23*(4), 4494-4505.

Karamdel, J., Dee, C. F., and Majlis, B. Y. (2011). Effects of annealing conditions on the surface morphology and crystallinity of sputtered ZnO nano films. *Sains Malaysiana, 40*(3), 209-213.

Kley, E.-B. (1997). Continuous profile writing by electron and optical lithography. *Microelectronic Engineering, 34*(3), 261-298.

Li, P., Xie, J., Cheng, J., and Jiang, Y. N. (2015). Study on weak-light photovoltaic characteristics of solar cell with a microgroove lens array on glass substrate. *Optics Express, 23*(7), A192-A203.

Majumdar, S. N., and Comtet, A. (2005). Airy distribution function: from the area under a Brownian excursion to the maximal height of fluctuating interfaces. *Journal of statistical physics, 119*(3-4), 777-826.

Nurul, I. A. R., and Ahmad, M. (2006). Transduser optik hidrogen peroksida berasaskan enzim peroksidase terpegun dalam Monolit hibrid sol-gel-kitosan. *Sains Malaysiana, 35*(1), 7-10.

Raith Softsware. (2007). Raith; Innovative Solutions for Nanofabrcation And Semiconductor Navigations [on-line]. Retrieved 20/0202014, from Raith GmbH and Raith USA, Inc. on www.raith.com

Tsui, C.-C., Wei, H.-C., Chang, W.-F., and Su, G.-D. J. (2012). Design and fabrication of a mid-wavelength infrared Fresnel lens via liquid poly (methyl methacrylate). *Journal of Micromechanics and Microengineering, IOP Publishing Ltd, 22*(4), 045010.

Xie, J., Wu, K., Cheng, J., Li, P., and Zheng, J. (2015). The micro-optic photovoltaic behavior of solar cell along with microlens curved glass substrate. *Energy Conversion and Management, 96*, 315-321.

Yu, Y.-H., Tian, Z.-N., Jiang, T., Niu, L.-G., and Gao, B.-R. (2015). Fabrication of large-scale multilevel phase-type Fresnel zone plate arrays by femtosecond laser direct writing. *Optics Communications*.